ЖУРНАЛ СТРУКТУРНОЙ ХИМИИ

2010. Том 51, № 3 *Май – июнь* *С. 593 – 597*

КРАТКИЕ СООБЩЕНИЯ

UDC 539.19;547-32

THEORETICAL STUDIES ON THE MECHANISM OF CHLORINATION REACTION OF TRICHLOROGERMYL ACRYLIC ACID

© 2010 **Y.Z. Fang[1,2], W.Y. Ma[1]*, J.H. Zhou[1], Y. Liu[2]**

[1]*Department of Chemical Engineering, Shandong Institute of Light Industry, Shandong Province, Jinan 250353, P. R. China*

[2]*Department of Catalysis Sciences and Technology, School of Chemical Engineering, Tianjin University, Tianjin 300072, P. R. China*

Received December, 4, 2008

The mechanism of the chlorination reaction of trichlorogermyl acrylic acid has been studied systematically using quantum chemistry methods. Geometries of reactants, transition states and products have been optimized at the B3LYP/6-311G(*d*,*p*) level. Vibrational frequencies, IR intensities and relative energies for various stationary points have been determined. The reaction pathways have been identified by intrinsic reaction coordinate (IRC) calculations. Theoretical analysis provides conclusive evidence that the process proceeds through two and three pathways for the first and second reaction steps, respectively.

K e y w o r d s: Germyl, crylic acid, density functional theory, potential energy calculations, transition state.

Carboxyethylgermanium sesquioxide [1—3] has potential antitumor activities and a lower level of toxicity compared with other pharmaceuticals, especially the forms of bis-β-carboxyethyl organogermanium sesquioxide $(GeCH_2CH_2COOH)_2O_3$ (R-Ge-1) and bis-β-carbamylethyl organogermanium sesquioxide $(GeCH_2CH_2CONH_2)_2O_3$ (R-Ge-2). Their therapeutic attributes include immunity enhancement, oxygen enrichment, free radical scavenging, analgesia and heavy metal detoxification. In our previous papers [4—6], we have reported three important reactions involved in the synthesis processes of R-Ge-1 using *ab initio* electronic calculations and the density functional theory. The chlorination reaction of trichlorogermyl acrylic acid is an essential step in preparing bioactive organic germaniums. Our objective of embarking on the present work is to conduct a systematic theoretical study of trichlorogermyl acrylic acid chlorination. Now this part of work is completed by quantum chemistry calculations. Geometries, energies, vibrational frequencies of reactants, products, and transition states (TSs) are obtained, and we hope these results will be valuable for better understanding the reaction mechanism for the R-Ge-2 system.

COMPUTATIONAL METHODS

Density functional theory [7, 8] was employed to calculate the potential energy surface for the chlorination reaction of trichlorogermyl acrylic acid. The geometries of all reactants, products and transition states were optimized at the B3LYP/6-311G(*d*,*p*) level. The corresponding harmonic vibrational frequencies were calculated at the same level in order to verify whether the stationary points were local minima or saddle points. The transition states were verified to connect with the designated reactants and products by performing intrinsic reaction coordinate (IRC) analysis. All the calculations above were performed by using the Gaussian 03 program suite [9]; some of them were carried out in

* E-mail: mawy@sdili.edu.cn

Virtual Laboratory of Computational Chemistry, Computer Network Information Center of Chinese Academy of Sciences.

RESULTS AND DISCUSSION

The chlorination reaction of trichlorogermyl acrylic acid comprises two processes:

$$GeCl_3CH_2CH_2COOH + SOCl_2 \rightarrow GeCl_3CH_2CH_2COCl + SOClOH \quad (r1)$$

$$GeCl_3CH_2CH_2COOH + SOClOH \rightarrow GeCl_3CH_2CH_2COCl + SO(OH)_2 \quad (r2)$$

Geometric parameters for the reactants, products, and the transition states optimized at the B3LYP/6-311G(*d*,*p*) level are displayed in Fig. 1. As shown in Fig. 1, we obtained the geometries of reactants for the equilibrium conformation of $GeCl_3CH_2CH_2COOH$ [R1] and $SOCl_2$ [R2], the corresponding geometries of products for the equilibrium conformation of $GeCl_3CH_2CH_2COCl$ [P1],

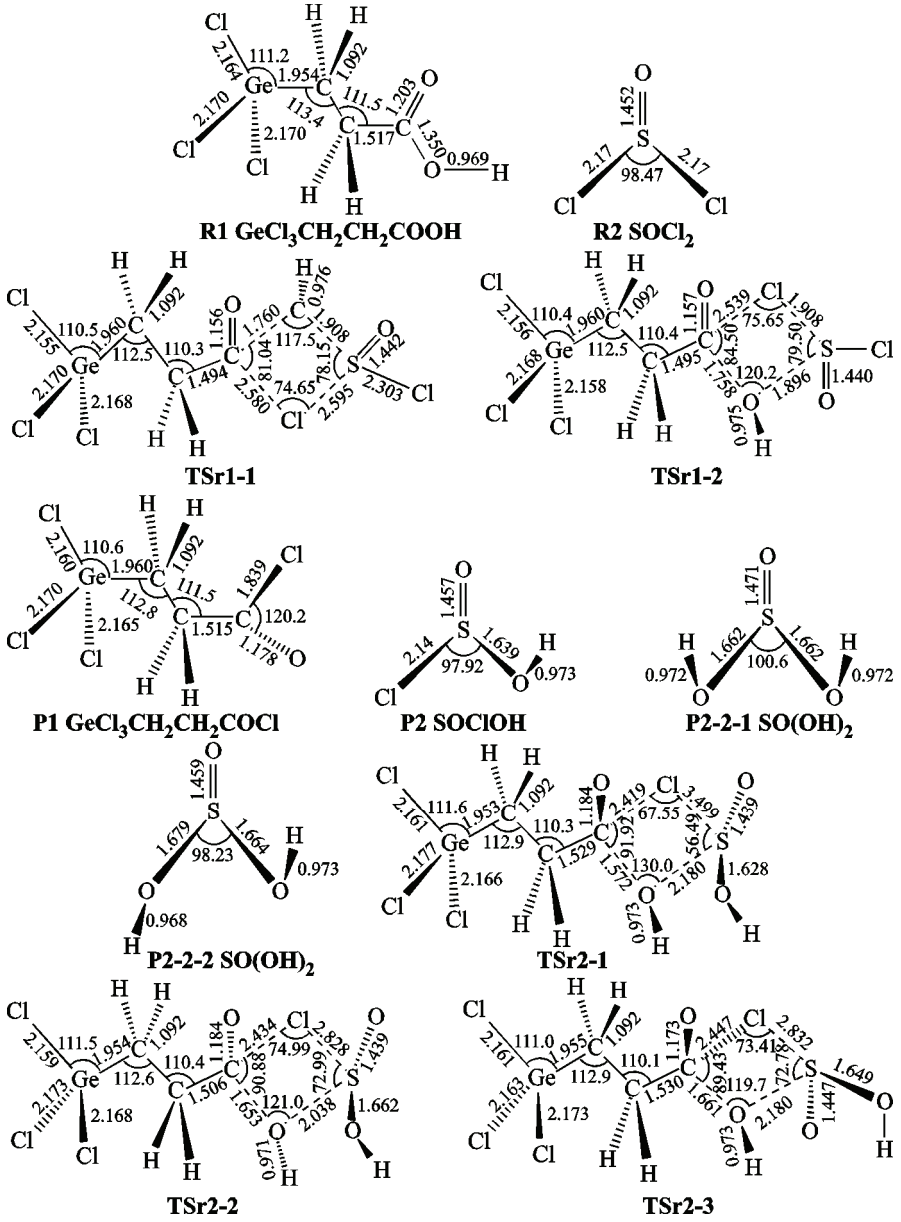

Fig. 1. The optimized B3LYP/6-311G(*d*,*p*) geometrical parameters for the stationary points on the potential energy surface. The distances are in Ångströms, the angles are in degrees

Table 1

Total energies E (*in Hartrees*) *and relative energies* E_{rel} (in kJ/mol) *of the investigated molecular structures* (see Figure 1)

Species	*E*	Species	*E*	Species	E_{rel}	Species	E_{rel}
R1	–3725.70116	P2-1	–1009.48715	R1+R2	0	TSr2-1	219.5223
R2	–1393.86305	TSr2-1	–4735.10469	TSr1-1	162.5421	TSr2-2	184.668
TSr1-1	–5119.50230	TSr2-2	–4735.11797	TSr1-2	158.9068	P1+P2-2-1	66.50514
TSr1-2	–5119.50368	P2-2-1	–625.10357	P1+P2-1	46.36674	P1+P2-2-2	72.13465
P1	–4110.05940	P2-2-2	–625.10143	R1+P2-1	0	—	—

SOClOH [P2-1] and $SO(OH)_2$ [P2-2-1, P2-2-2]. Furthermore, we also detected five transition states [TSr1-1, TSr1-2, TSr2-1, TSr2-2, TSr2-3] for the title reaction. The five possible reaction pathways are:

$$R1+R2 \rightarrow TSr1\text{-}1 \rightarrow P1+P2\text{-}1;$$

$$R1+R2 \rightarrow TSr1\text{-}2 \rightarrow P1+P2\text{-}1;$$

$$R1+P2\text{-}1 \rightarrow TSr2\text{-}1 \rightarrow P1+P2\text{-}2\text{-}1;$$

$$R1+P2\text{-}1 \rightarrow TSr2\text{-}2 \rightarrow P1+P2\text{-}2\text{-}2;$$

$$R1+P2\text{-}1 \rightarrow TSr2\text{-}3 \rightarrow P1+P2\text{-}2\text{-}2.$$

The calculated total energies for transition states, reactants and products for the title reaction are listed in Table 1. From Table 1, we can see that all the activation energies for r1 are lower than that for r2; in other words, the first chlorine atom of thionyl chloride can attack the hydroxyl group of trichlorogermyl acrylic acid much easier than the second one. The order of kinetic stability of these four transition states is

$$TSr1\text{-}2 > TSr1\text{-}1 > TSr2\text{-}2 > TSr2\text{-}1.$$

The activation barriers for the reaction channels are 158.9068, 162.5421, 184.668, 219.5223 kJ/mol, respectively.

Frequency calculations were carried out for all the reactants, products, and transition states. The most intense vibrational frequencies are listed in Table 2. In the IR spectra of R1, TSr1-1, TSr1-2, P1, TSr2-1, TSr2-2 and TSr2-3, the C=O symmetric stretching bands are situated in the range of 1829—1940 cm^{-1}. For transition states, the character of the stationary points was confirmed by normal-mode

Table 2

Harmonic vibrational frequencies with stronger IR intensity for structures calculated at B3LYP/6-311G(*d*,*p*) *level*

Species	Vibrational frequencies (cm^{-1})
R1	1829 1147 414 1216 1147 660 3757 1404 723 407 1157 382 1051 3757
R2	406 1240 453 257 312 168
TSr1-1	–248 2044 481 169 382 390 927 151 927 551 3670 1093 738 732
TSr1-2	–290 2036 491 925 1278 3684 524 203 383 341 1074 190 734
P1	1894 595 1004 419 412 1023 1181 734 566 427 387 942 710
P2-1	471 744 1235 3705 435 1086 271 215 325
TSr2-1	–368 1869 780 951 335 415 3719 3713 1036 1285 1036 405 934
TSr2-2	–283 1929 697 515 950 1046 260 282 3746 3694 418 763 406
TSr2-3	–295 715 1940 501 949 3713 1265 3700 419 212 590 278 408
P2-2-1	716 726 1219 428 3709 427 1066 3707 468 174 311 1092
P2-2-2	629 724 1241 1068 278 3769 457 3704 228 469 1095 379

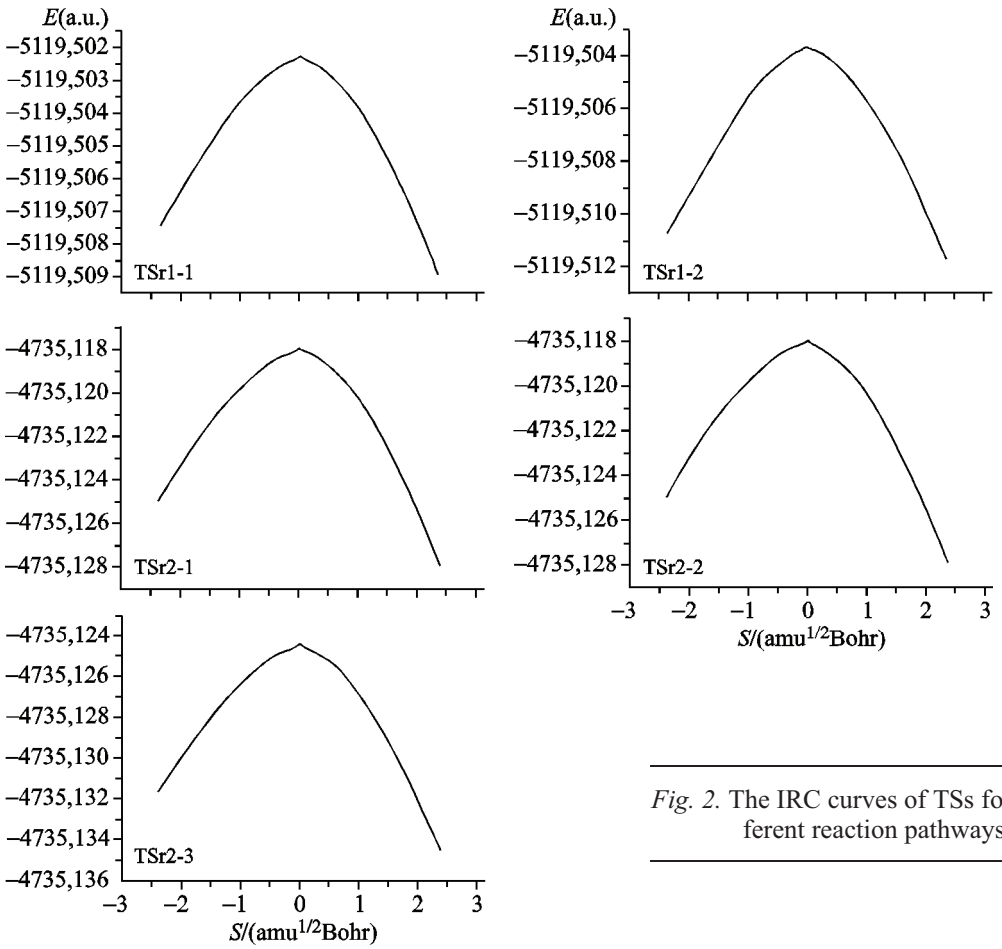

Fig. 2. The IRC curves of TSs for the different reaction pathways

analysis, which yielded one and only one imaginary frequency (248i, 290i, 368i, 283i and 295i) whose eigenvectors correspond to the direction of the reaction. On the other hand, all the optimized stable structures have positive frequencies.

In order to confirm the reaction mechanism and to characterize the nature of the transition states, the intrinsic reaction coordinate (IRC) calculations were performed by using the same level. The IRC curves of TSs for the different reaction pathways are shown in Fig. 2.

Vibrational analysis and IRC calculations indicate that both TSr1-1 and TSr1-2 connect the reactants R1+R2 and the products P1+P2-1; TSr2-1 connects the reactants R1+P2-1 and the products of P1+P2-2-1; TSr2-2 and TSr2-3 connect the reactants R1+P2-1 and P1+P2-2-2. The overall profile of the potential energy surface is presented in Fig. 3.

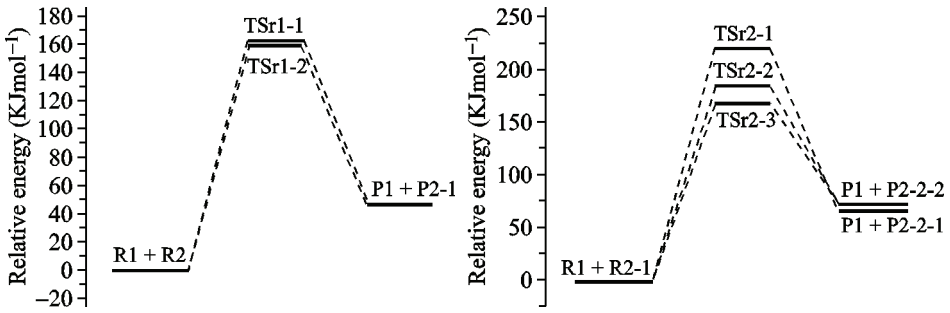

Fig. 3. Potential energy surface (PES) of the reaction

For the two reaction steps proposed in this work, the transition state of TSr1-2 in reaction r1 is favored kinetically, *i.e.* the formation of product from the reactant occurs easily; at the same time, the reaction pathway *via* the transition state TSr2-3 is the main one in the reaction r2.

CONCLUSIONS

We have thoroughly explored the title reaction by DFT method at B3LYP/6-311G(*d*,*p*) level. The systematic calculations of this study can qualitatively explain the complicated behavior of the whole reaction comprising the two processes: r1 and r2. We obtained the stable equilibrium structures of reactants and products of the title reaction, and two kinds of TSs involved in r1 and three kinds of TSs involved in r2. The reaction mechanism is reported in detail; for the two steps r1 and r2, the dominating reaction pathways are R1+R2 → TSr1-2 → P1+P2-1 and R1+P2-1 → TSr2-3 → P1+P2-2-2, respectively.

This project was supported by the Natural Science Foundation of Shandong Province (N Y2008B33).

REFERENCES

1. *Barofsky D.F., Baum E.J.* // J. Amer. Chem. Soc. – 1976. – **98**, N 25. – P. 8287 – 8289.
2. *Nakada Y., Kosaka T., Kuwabara M. et al.* // J. Vet. Med. Sci. – 1993. – **55**, N 5. – P. 795 – 799.
3. *Schauss G.* // Biol. Trace Elem. React. – 1991. – **29**, N 3. – P. 267 – 280.
4. *Fang Y.Z., Ma W.Y., Zhou J.H. et al.* // J. Mol. Struct. (Theochem). – 2008. – **857**. – P. 51 – 56.
5. *Fang Y.Z., Chuan L., Zhou J.H. et al.* // Chin. Chem. Lett. – 2008. – **19**. – P. 493 – 496.
6. *Fang Y.Z., Ma W.Y., J. Zhang et al.* // Mol. Simulat. – 2008. – **34**, N 5. – P. 533 – 540.
7. *Lee T., Yang W.T., Parr R.G.* // Phys. Rev. B. – 1988. – **37**, N 2. – P. 785 – 789.
8. *Becke D.* // J. Chem. Phys. – 1993. – **98**. – P. 5648 – 5652.
9. *Frisch M.J., Trucks G.W., Schlegel H.B. et al.* Gaussian 03, Revision D.01, Gaussian, Inc., Wallingford CT, 2004.